Progress In Electromagnetics Research, PIER 101, 33–42, 2010

NOVEL PLANAR MULTIMODE BANDPASS FILTERS WITH RADIAL-LINE STUBS

L. Zhang, Z.-Y. Yu, and S.-G. Mo

Institute of Applied Physics
University of Electronic Science and Technology of China
Chengdu 610054, China

Abstract—This paper presents a novel approach for designing planar multimode wideband bandpass filters with good selectivity. The multimode resonator is composed of an open-ended microstrip line with length of half-wavelength ($\lambda/2$) and several radial-line stubs. By using different kinds of radial-line loaded stubs, different kinds of responses including three-pole and four-pole bandpass filters can be realized. Depending on electric field distribution and equivalent circuit model, the characteristics of the filter are analyzed. To verify the proposed method, two filters are implemented. The measured results exhibit good agreement with the simulation.

1. INTRODUCTION

With the development of wireless communication systems, microwave bandpass filters with compact size and high performance are highly desired. They are widely studied, and different kinds of bandpass filters have been proposed [1–14]. To make the filters more compact, one of the effective ways is to modify the traditional resonator to generate additional modes, causing the resonator to have multiple resonant frequencies, thus one resonator in physical can be treated as multiple resonators in electrical [9]. In [10], the design of dual-mode filter using a $\lambda/2$ center stub-loaded resonator is introduced. A $\lambda/2$ transmission line resonator with a pair of center loaded stubs is used to design triple-mode filters [11–13]. All this kind of filters using stub-loaded structure have a good selectivity for the transmission zeros are close to the passband. The radial-line stubs have been found to work better than low impedance rectangular stubs when an accurate localization of a zero-point impedance is needed, and it can maintain

Corresponding author: L. Zhang (angong1985@163.com).

the lower impedance level over a wide frequency range and a smaller outer dimension [14, 15].

In this article, the design of planar multimode bandpass filters is investigated. Compared to the traditional stub-loaded filters presented in [11, 12], a wider passband can be obtained for the introduction of radial-line stubs, and the frequencies of each mode can be controlled by the radii of the radial-line stubs easily. For different kinds of radial-line stubs loading, the three- and four-pole bandpass filters are designed and studied respectively. Finally, two filters are fabricated and measured to validate the design.

2. THREE-POLE BANDPASS FILTER

2.1. Design and Analysis

As illustrated in Figure 1, a $\lambda/2$ microstrip line resonator with length $2l$ is simultaneously loaded at its center point with a pair of radial-line stubs. The two radial-line stubs with the same angle θ but different radii are symmetrical with respect to the dashed line A-B. The resonator is fed by a pair of orthogonal $50\,\Omega$ microstrip lines, and each microstrip line is connected to a coupling arm. The filter is fabricated on the substrate of Rogers TMM 10 with thickness of $h = 1\,\text{mm}$ and relative permittivity of $\varepsilon_r = 9.2$. The structural parameters are as follows: $w = 0.4\,\text{mm}$, $w_1 = 1\,\text{mm}$, $g = 0.2\,\text{mm}$, $l = 15.1\,\text{mm}$, $l_1 = 11.1\,\text{mm}$, $\theta = 30\,\text{deg}$, $r_1 = 15.4\,\text{mm}$, $r_2 = 7.7\,\text{mm}$.

A commercially available full-wave electromagnetic simulator is used to characterize the frequency response of the three-pole filter. By

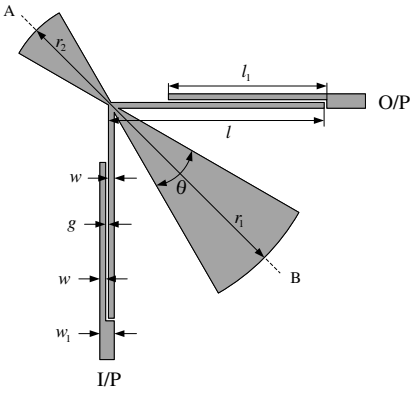

Figure 1. Layout of proposed three-pole filter.

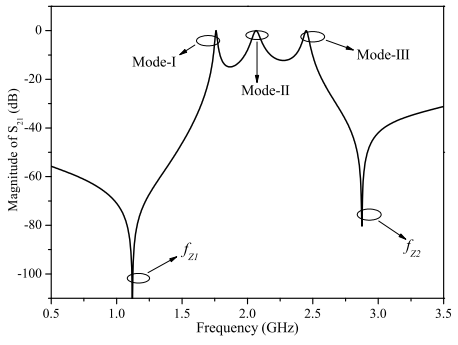

Figure 2. Mode resonant characteristic of the three-pole resonator.

using weak coupling, the simulated result is plotted in Figure 2. As can be seen, three modes and two transmission zeros are obtained for the filter. Figure 3 illustrates the electric field distribution for the three modes in the substrate, respectively. It is obvious that the Mode-II have an electric field distribution only within the $\lambda/2$ microstrip line, while the other two modes have an electric field distribution both within the $\lambda/2$ microstrip line and radial-line stubs. It is also need to notice that there is a little electric field distribution within the larger radial-line stubs for Mode-III. So the frequency of Mode-II can be approximately expressed as [10]:

$$f_c = \frac{c}{4l\sqrt{\varepsilon_e}} \tag{1}$$

where c is the velocity of light in free space, and ε_e represents the effective permittivity of the substrate. It can be seen from (1) that the center resonant frequency of the fist passband can be controlled by tuning the size of parameter l.

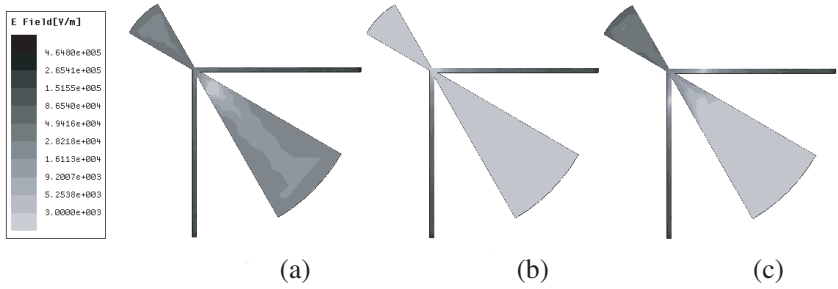

Figure 3. Electric field distribution. (a) Mode-I. (b) Mode-II. (c) Mode-III.

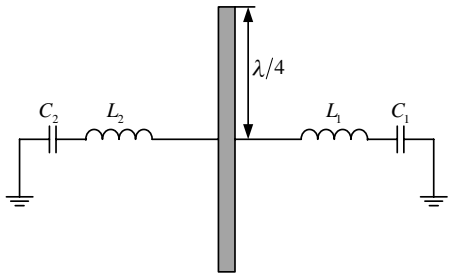

Figure 4. Equivalent circuit model of the proposed resonator.

Figure 4 is an equivalent circuit model of the proposed resonator. The two radial-line stubs are equivalent to two series LC resonant circuits. So the resonant frequencies of the two series LC circuits can be expressed as:

$$f_1 = \frac{1}{2\pi\sqrt{L_1 C_1}} \tag{2}$$

$$f_2 = \frac{1}{2\pi\sqrt{L_2 C_2}} \tag{3}$$

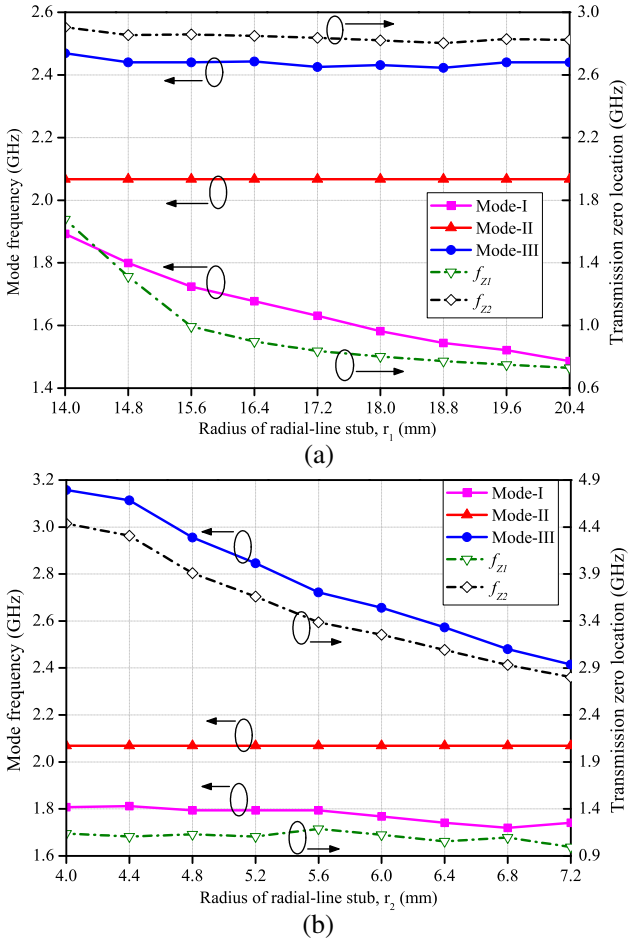

Figure 5. Simulated mode frequencies and transmission zero location. (a) Against radius r_1 of the larger radial-line stub for $r_2 = 7\,\text{mm}$. (b) Against radius r_2 of the smaller radial-line stub for $r_1 = 15.4\,\text{mm}$.

It can be considered that, for the resonance of the series LC circuits, the signal cannot be transmitted from source to load through the $\lambda/2$ microstrip line at frequencies f_1 and f_2, and two transmission zeros are obtained in the upper and lower stopbands of response respectively. The introduced transmission zeros can improve the selectivity of filter effectively. The resonant frequencies of series LC can be controlled by the radii of radial-line stubs r_1 and r_2. The simulated modal resonant frequencies and the position of transmission zeros against the radii of r_1 and r_2 are shown in Figure 5. As can be seen from the figures, for the electric field distribute only within $\lambda/2$ microstrip line for mode-II, its frequency keeps invariable when the radii of the radial-line stubs r_1 and r_2 are changed. In Figure 5(a), when r_1 increases from 14.0 mm to 20.4 mm, the frequency of Mode-I declines while the frequency of Mode-III nearly has no change. Meanwhile, with the increase of r_1, the equivalent inductance L_1 and capacity C_1 of the larger radial-line stub increase. From (2) we know the resonant frequency f_1 decreases, so the location of transmission zero f_{Z1} also declines while the location of transmission zero f_{Z2} nearly has no change. In Figure 5(b), when r_2 increases from 4.0 mm to 7.2 mm, the frequency of Mode-III declines while the frequency of Mode-I nearly has no change. Meanwhile, the location of transmission zero f_{Z2} also declines while the location of transmission zero f_{Z1} nearly has no change.

From above analysis we can get that Mode-I and transmission zero f_{Z1} are mainly controlled by the radius r_1 of the larger radial-line stub; Mode-III and transmission zero f_{Z2} are mainly controlled by the radius r_2 of the smaller radial-line stub; Mode-II is determined by the length of the $\lambda/2$ microstrip line. It provides a convenient way to design the three-pole bandpass filter with good selectivity.

2.2. Simulated and Experimental Results

Depending on the discussion above, a three-pole bandpass filter is fabricated, as shown in Figure 6(a). The simulated and experimental frequency responses of the proposed three-pole filter are shown in Figure 6(b). The simulated results show that the triple-mode filter operated at 2.0 GHz has a 3 dB fractional bandwidth of 30.6%. A pair of transmission zeros are located at 1.58 GHz with 49.37 dB attenuation and 2.76 GHz with 52.42 dB attenuation respectively, which provide a better cutoff rate in the stopband and improve the selectivity. The measured minimum insertion loss is about 1.13 dB in the passband, which is mainly due to the conductor and dielectric losses of the substrate. The simulated results agree with the measured ones. Some discrepancies between them are mainly due to the inaccuracy in fabrication.

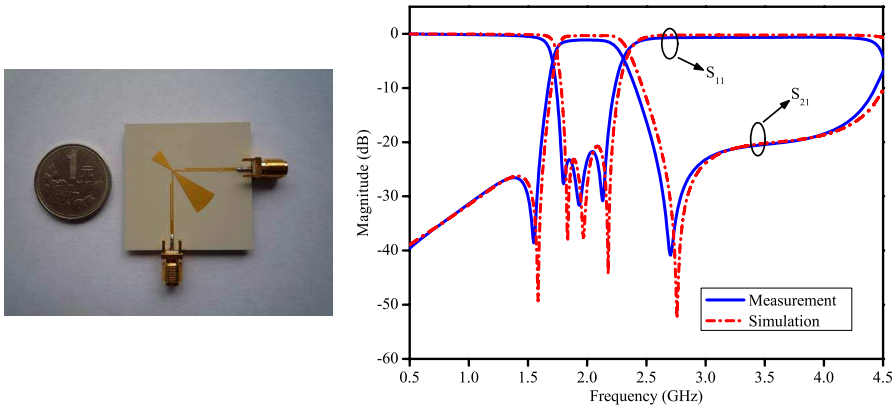

Figure 6. (a) Photograph of the fabricated filter. (b) Measured and simulated frequency responses of the filter.

3. FOUR-POLE BANDPASS FILTER

3.1. Design and Analysis

In Section 2, the $\lambda/2$ microstrip line resonator is simultaneously loaded by two radial-line stubs, so a three-pole bandpass filter is realized. In this section, to realize a four-pole bandpass filter, the $\lambda/2$ microstrip line resonator with length $2l$ is simultaneously loaded by three radial-line stubs with the same angle θ. First, a modified three-pole bandpass filter is shown in Figure 7(a). The resonator is symmetrical with respect to the dashed line A-B, and two radial-line stubs with the same radius are connected symmetrically to the $\lambda/2$ microstrip line but with distance s apart. Figure 7(b) is the proposed four-pole filter. Compared with the modified three-pole bandpass filter, a larger radial-line stub is introduced at the center point of the $\lambda/2$ microstrip line. The resonator is fed by a pair of orthogonal $50\,\Omega$ microstrip lines, and each microstrip line is connected to a coupling arm. The filter is fabricated on the substrate of Rogers TMM 10 with thickness of $h = 1\,\text{mm}$ and relative permittivity of $\varepsilon_r = 9.2$. The structural parameters are as follows: $w = 0.4\,\text{mm}$, $w_1 = 1\,\text{mm}$, $g = 0.2\,\text{mm}$, $l = 15\,\text{mm}$, $l_1 = 11.2\,\text{mm}$, $\theta = 30\,\text{deg}$, $s = 1.5\,\text{mm}$, $r_1 = 14.2\,\text{mm}$, $r_2 = 8\,\text{mm}$.

The simulated frequency responses of the two filters in Figure 7 are shown in Figure 8. For the modified three-pole filter, both the transmission zeros as the first filter example in Part 2 are located at

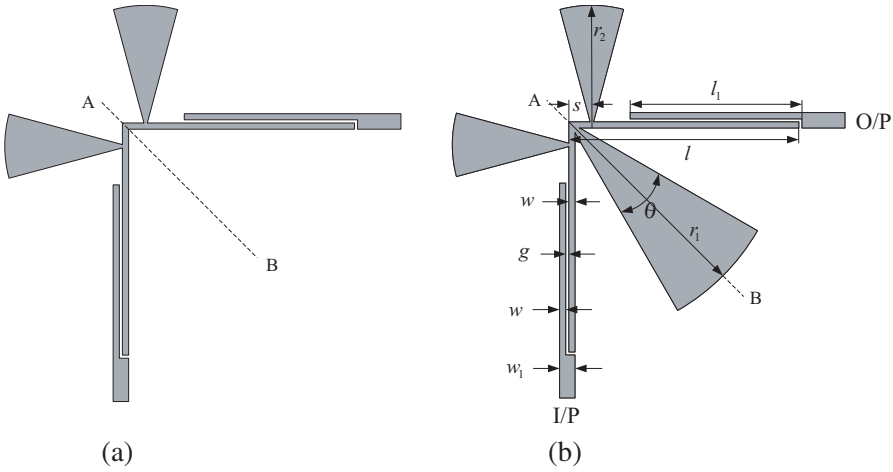

Figure 7. (a) Layout of modified three-pole filter. (b) Layout of proposed four-pole filter.

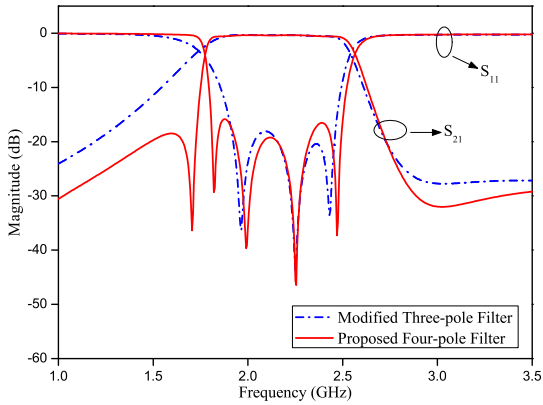

Figure 8. Simulated frequency responses of modified three-pole filter and four-pole filter.

the upper stopband and merged. There is no transmission zero in the lower stopband. As analysis in Section 2, each radial-line stub loaded at the center point of the $\lambda/2$ microstrip line can be used to introduce one mode and a transmission zero. So compared with the modified three-pole bandpass filter, the four-pole bandpass filter not only adds a pole, but also adds a transmission zero. The passband is widened, and the selectivity of the lower stopband is improved.

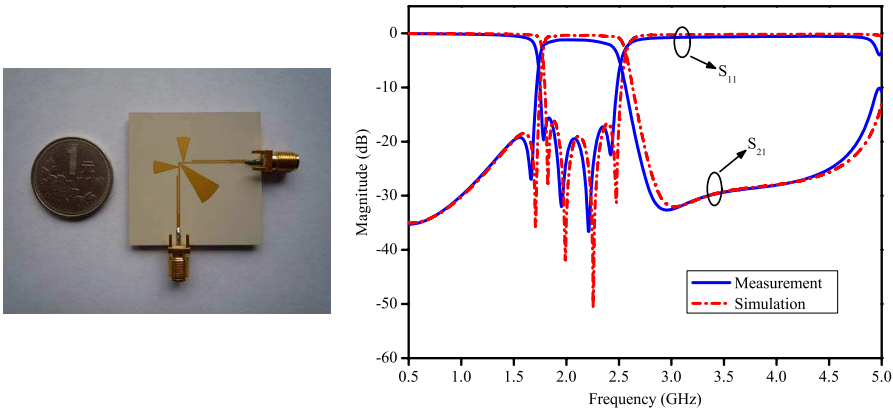

Figure 9. (a) Photograph of the fabricated four-pole filter. (b) Measured and simulated frequency responses of the filter.

3.2. Simulated and Experimental Results

To verify the design, a four-pole bandpass is fabricated, as shown in Figure 9(a). The simulated and experimental frequency responses of the proposed three-pole filter are shown in Figure 9(b). The simulated results show that the four-pole filter operated at 2.17 GHz has a 3 dB fractional bandwidth of 36.4%. A transmission zero is located at 1.705 GHz with 36.375 dB attenuation, which can improve the selectivity out of band. The measured minimum insertion loss is about 1.2 dB in the passband, which is mainly due to the conductor and dielectric losses of the substrate. Simulated and measured results have a good agreement.

4. CONCLUSION

A novel approach for designing planar three-pole and four-pole wideband bandpass filters is presented in this article. For the using of radial-line stubs, the design of filters is easy and accurate, and a wide passband can be obtained. Associated with electric field distribution and equivalent circuit model, the characteristics of three-pole bandpass filter are investigated. Then, by changing the location and number of radial-line stub-loaded, a four-pole bandpass filter is realized. Two experimental filters are fabricated to verify the design. A good agreement is obtained between simulation and measurement.

ACKNOWLEDGMENT

This work is supported by the National Natural Science Foundation of China (NSFC) under grant 60871058.

REFERENCES

1. Mo, S.-G., Z.-Y. Yu, and L. Zhang, "Design of triple-mode bandpass filter using improved hexagonal loop resonator," *Progress In Electromagnetics Research*, PIER 96, 117–125, 2009.
2. Xiao, J.-K., Q.-X. Chu, and H.-F. Huang, "Novel microstrip right-angled triangular patch resonator bandpass filter," *Journal of Electromagnetic Waves and Applications*, Vol. 22, No. 4, 581–591, 2008.
3. Wang, J.-P., L. Wang, Y.-X. Guo, Y. X. Wang, and D.-G. Fang, "Miniaturized dual-mode bandpass filter with controllable harmonic response for dual-band applications," *Journal of Electromagnetic Waves and Applications*, Vol. 23, No. 11–12, 1525–1533, 2009.
4. Zhao, L.-P., C.-H. Liang, G. Li, and X.-W. Dai, "Novel design of dual-mode bandpass filter with triangular structure," *Journal of Electromagnetic Waves and Applications*, Vol. 22, No. 7, 923–932, 2008.
5. Wu, G.-L., W. Mu, X.-W. Dai, and Y.-C. Jiao, "Design of novel dual-band bandpass filter with microstrip meander-loop resonator and CSRR DGS," *Progress In Electromagnetics Research*, PIER 78, 17–24, 2008.
6. Mo, S.-G., Z.-Y. Yu, and L. Zhang, "Compact dual-mode bandpass filters using hexagonal meander loop resonators," *Journal of Electromagnetic Waves and Applications*, Vol. 23, No. 13, 1723–1732, 2009.
7. Zhao, L.-P., X. Zhai, B. Wu, T. Su, W. Xue, and C.-H. Liang, "Novel design of dual-mode bandpass filter using rectangle structure," *Progress In Electromagnetics Research B*, Vol. 3, 131–141, 2008.
8. Serrano, A. L. C. and F. S. Correra, "A triple-mode bandpass filter using a modified circular patch resonator," *Microw. Opt. Technol. Lett.*, Vol. 51, No. 1, 178–182, 2009.
9. Hong, J.-S. and M. J. Lancaster, *Microstrip Filters for RF/Microwave Applications*, Wiley, New York, 2001.
10. Zhang, X. Y., J.-X. Chen, Q. Xue, and S.-M. Li, "Dual-band

bandpass filters using stub-loaded resonators," *IEEE Microw. Wireless Compon. Lett.*, Vol. 17, No. 8, 583–585, 2007.

11. Zhu, L. and W. Menzel, "Compact microstrip bandpass filter with two transmission zeros using a stub-tapped half-wavelength line resonator," *IEEE Microw. Wireless Compon. Lett.*, Vol. 13, No. 1, 16–18, 2003.
12. Amari, S., K. Hamed, Y. Antar, and A. Freundorfer, "New elliptic microstrip $\lambda/4$-resonator filters," *Proc. Asia-Pacific Microw. Conf.*, 755–758, 2001.
13. Li, L., Z.-F. Li, and Q.-F. Wei, "A quasi-elliptic wideband bandpass filter using a novel multiple-mode resonator constructed by an asymmetric compact microstrip resonant cell," *Microw. Opt. Technol. Lett.*, Vol. 51, No. 3, 713–714, 2009.
14. Giannini, F., R. Sorrentino, and J. Vrba, "Planar circuit analysis of microstrip radial stub," *IEEE Trans. Microw. Theory Tech.*, Vol. 32, No. 12, 1652–1655, 1984.
15. Ma, K., K. S. Yeo, and Q. Sun, "A novel planar multimode bandpass filter with radial perturbation," *Microw. Opt. Technol. Lett.*, Vol. 51, No. 4, 964–966, 2009.